Contents lists available at ScienceDirect

Environmental Modelling and Software

journal homepage: www.elsevier.com/locate/envsoft

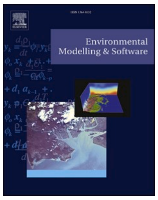

A CUDA Fortran GPU-parallelised hydrodynamic tool for high-resolution and long-term eco-hydraulic modelling

Marcos Sanz-Ramos [a,*], David López-Gómez [b], Ernest Bladé [a], Danial Dehghan-Souraki [a]

[a] Flumen Institute, Universitat Politècnica de Catalunya (UPC), International Center for Numerical Methods in Engineering (CIMNE), 08034, Barcelona, Spain
[b] Centro de Estudios Hidrográficos, Centro de Estudios y Experimentación de Obras Públicas (CEDEX), 28005, Madrid, Spain

ARTICLE INFO

Handling Editor: Daniel P Ames

Keywords:
Fish habitat
Weight useable area
Numerical modelling
High performance computing
GPGPU

ABSTRACT

Eco-hydraulic models are wide extended tools to assess physical habitat suitability on aquatic environments. Currently, the application of these tools is limited to short river stretches and steady flow simulations. However, this limitation can be overcome with the application of a high-performance computing technique: graphics processing unit (GPU) computing. R-Iber is a GPU-based hydrodynamic code parallelised in CUDA Fortran that, with the integration of a biological module, performs as an eco-hydraulic numerical tool. R-Iber was validated and applied to real cases by using an optimised instream flow incremental methodology in long river reaches and long-term simulations. R-Iber reduces the computation time considerably, reaching speed-ups of two orders of magnitude compared to traditional computing. R-Iber allows for overcoming the current limitations of the eco-hydraulic tools with the simulation of high-resolution numerical models calculated in a reasonable computation timeframe, which provides a better representation of the hydrodynamics and the physical habitat.

Software availability

- Name of tool: R-Iber
- Developers: David López-Gómez, Marcos Sanz-Ramos, Ernest Bladé.
- Year first available: 2021.
- Hardware required: basic computer with a graphical power unit (GPU) based on CUDA architecture (mainly, any NVIDIA GPU).
- Requirements: Windows OS x64.
- Source Code Availability: the numerical tool is freely distributed through www.iberaula.com
- Data availability: the authors do not have permissions to share the data.
- Cost: free
- Program languages: CUDA Fortran

1. Introduction

Water resources and river management are no longer uniquely related to flood or drought scenarios. On the contrary, to properly study the system from a holistic point of view, the relationship between hydraulics and biota must be considered (Benjankar et al., 2018; Palau and Alcázar, 2012; Wilkes et al., 2016) in all situations, not only during extreme conditions.

Eco-hydraulics is a technique that analyses the effect of physical environmental properties (flow depth, velocity, turbulence, temperature, substrate, etc.) on aquatic environments (Bovee, 1982), such as rivers. To characterise the physical habitat, several approaches have been proposed based on hydrologic, geomorphologic or hydraulic criteria (Tonina and Jorde, 2013). Particularly for hydraulics, a common method for assessing physical habitat is the use of normalized univariate curves, or suitability curves, that relate variables of the river environment with the inhabiting species' use of the space.

Several numerical hydrodynamic tools have been developed or enhanced by integrating the biological requirements of one or several target species typically of fishes (Cassan et al., 2022; Hung et al., 2022; Jowett, 2004; Meza Rodríguez et al., 2019; Nones, 2019; Sanz-Ramos et al., 2019; Shim et al., 2020; Stamou et al., 2018; Steffler and Blackburn, 2002), but not exclusively (Hamilton et al., 2015; Zohmann et al., 2013). These tools are based on the solution of the one-dimensional (1D), and most recently, on the two-dimensional (2D) Saint-Venant equations or shallow water equations (SWE), which provide the evolution of the water depth and the specific discharge or velocity of the

Abbreviations: SWE, shallow water equations; HPC, high-performance computing; GPGPU, general-purpose computing on graphics processing unit; GPU, graphics processing unit; CPU, central processing unit; CUDA, compute unified device architecture; IFIM, instream flow incremental methodology; WUA, weight usable area.

* Corresponding author.

E-mail addresses: marcos.sanz-ramos@upc.edu (M. Sanz-Ramos), ernest.blade@upc.edu (E. Bladé), danial.dehghan@upc.edu (D. Dehghan-Souraki).

https://doi.org/10.1016/j.envsoft.2023.105628
Received 11 August 2022; Received in revised form 9 January 2023; Accepted 10 January 2023
Available online 14 January 2023

water. Despite the current rapid increase in the use of three-dimensional (3D) river flow modelling (Bermúdez et al., 2017, 2018; Meselhe et al., 2012; Pisaturo et al., 2017), the computational cost of this method limits its application to very short river stretches and research purposes.

Apart from the simplifications applied to the generation of the suitability curves (Boudreault et al., 2022; Palau et al., 2016), limitations of 2D-SWE-based eco-hydraulic models typically relate to computational cost (Carlotto et al., 2021; Morales-Hernández et al., 2021). The time required to simulate large river stretches, flow properties in natural conditions (e.g. long time series), and the use of a very fine domain discretisation with thousands or millions of calculation points (or mesh elements) typically require high computational effort.

These limitations can be overcome with a good code design or/and with the application of high-performance computing (HPC) techniques. Currently, one of the most applied techniques is the parallelisation of the computations by using general-purpose computing on graphics processing unit (GPGPU) instead of the traditional central processing unit (CPU) computing (Buttinger-Kreuzhuber et al., 2022; Carlotto et al., 2021; Morales-Hernández et al., 2021).

A GPGPU technique commonly used in computational fluid dynamics (CFD) is that provided by the NVIDIA compute unified device architecture (CUDA), which is currently available for the C++ and Fortran programming languages (NVIDIA, 2022a). The benefit of using GPU computing is the significant reduction in computation time, with speed-ups of one or two orders of magnitude compared to CPU computing. Nevertheless, 2D-SWE-based eco-hydraulic numerical tools that include an integrated GPU-parallelised hydrodynamic module and physical habitat module are lacking.

This study aims to fill this gap with the presentation of a new GPU-based hydraulic code parallelised in CUDA Fortran, named R-Iber, and its performance as an eco-hydraulic numerical tool with the integration of a physical habitat module. The code was first validated using two different benchmark tests for 2D-SWE-based models and a laboratory experiment with a vertical slot fishway. Then, R-Iber was applied to two real cases to show not only the full integration of the hydrodynamic and physical habitat module for some fish species but also the benefits of using a fully-integrated GPU-parallelised eco-hydraulic tool in high-resolution numerical models and long-term simulations.

2. Materials and methods

2.1. Governing equations

Most existing eco-hydraulic simulation tools are based on the solution of the mass and momentum conservation equations that, when applied to a 2D framework, are named 2D Shallow Water Equations (2D-SWE). They are derived from Navier–Stokes equations through a time averaging to filtrate the turbulent fluctuations (Reynolds Averaged Navier–Stokes equations [RANS]) and a depth averaging to obtain the final 2D equations. Two-dimensional SWE are a hyperbolic nonlinear system of three differential equations in partial derivatives (Toro, 2009), which can be written as follows:

$$
\begin{aligned}
&\frac{\partial h}{\partial t}+\frac{\partial hU_x}{\partial x}+\frac{\partial hU_y}{\partial y}=0\\
&\frac{\partial hU_x}{\partial t}+\frac{\partial}{\partial x}\left(hU_x^2+g\frac{h^2}{2}\right)+\frac{\partial}{\partial y}\left(hU_xU_y\right)=gh\left(S_{o,x}-S_{f,x}\right)+\frac{\partial}{\partial x}\left(\nu_t h\frac{\partial U_x}{\partial x}\right)+\frac{\partial}{\partial y}\left(\nu_t h\frac{\partial U_y}{\partial y}\right)\\
&\frac{\partial hU_x}{\partial t}+\frac{\partial}{\partial y}\left(hU_xU_y\right)+\frac{\partial}{\partial y}\left(hU_y^2+g\frac{h^2}{2}\right)=gh\left(S_{o,y}-S_{f,y}\right)+\frac{\partial}{\partial x}\left(\nu_t h\frac{\partial U_y}{\partial y}\right)+\frac{\partial}{\partial y}\left(\nu_t h\frac{\partial U_y}{\partial y}\right)
\end{aligned}
\qquad [1]
$$

where h is the water depth, U_x and U_y are the x and y components of the depth-averaged velocity, g is the gravitational acceleration, $S_{o,x} = -\partial z_b/\partial x$ and $S_{o,y} = -\partial z_b/\partial y$ are the spatial variation of the bed elevation (z_b) on the x and y directions, $S_{f,x} = (n^2 U_x \sqrt{U_x^2 + U_y^2})/h^{4/3}$ and $S_{o,y} = (n^2 U_y \sqrt{U_x^2 + U_y^2})/h^{4/3}$ are the energy dissipation in the x and y directions due to bed friction, which is computed using the Manning formula, and ν_t is the turbulent viscosity.

The previous system of equations are the main part of the hydrodynamics module of Iber (Bladé et al., 2014a, 2014b), a 2D numerical tool that was initially developed for hydrodynamics and sediment transport modelling (Bladé et al., 2014a, 2014b, 2019b, 2019a; Sanz--Ramos et al., 2020a). It solves the 2D-SWE on irregular geometries using the conservative scheme based on the Finite Volume Method of Roe (1986), which consists of the Godunov method together with the Roe Approximate Riemann Solver (Toro, 2009). The tool has been continuously enhanced, and the sequential version currently includes a series of modules for different free surface flow processes, such as hydrological processes (Cea and Bladé, 2015; Sanz-Ramos et al., 2020b, 2021), pollutant propagation (Cea et al., 2016), large-wood transport (Ruiz--Villanueva et al., 2014), and physical habitat suitability assessment (Sanz-Ramos et al., 2019).

2.2. Eco-hydraulics methods

The combination of a hydrodynamic model and a biological model can be oriented to develop eco-hydraulic tools (Nestler et al., 2016). One of the most extended biological models to assess physical habitat, particular for freshwater fishes, is the use of suitability curves, a normalized relation between environmental variables (hydraulic, water quality, geomorphological, etc.) and the use of the space of the target specie/stadium. The elemental habitat suitability of a physical variable ranges from 0 to 1, values being close to 1 those correspond to a high degree of suitability. The multiplication of the elemental suitability (depth- and velocity-dependent) of each species/stadium was used as habitat criteria in the following sections, but other criteria can be used without loss of applicability.

The Instream Flow Incremental Methodology (IFIM) is a technique that uses the combination of hydrodynamic and biologic models to create a habitat or eco-hydraulic model. It consists of the assessment of different constant discharges (Q) in a river stretch to obtain the Weight Useable Area (WUA) for each one (Bovee, 1982). With these Q-WUA relations, it is possible to obtain the theoretical discharge that maximises the WUA for the species and stadiums analysed, and which is usually utilized to propose the environmental flows.

In 2D eco-hydraulic modelling, the use of the IFIM traditionally implies the generation of as many models as the discharges to be evaluated. Being an analysis conducted under steady flow conditions, 2D-SWE-based models usually require simulating the model from the beginning to an unknown maximum time of simulation. Additionally, the time required to achieve each steady state of the series of discharges to evaluate is, in general, unknown. This time depends not only on the geometry and length of the river, but also on the flow intensity. This issue is addressed with the definition of a series of constant discharges, or 'stepped discharges', as an inlet condition. The 'stepped discharge' option allows for computing, in a unique model, a series of discharges that generates steady conditions considering a tolerance between the inlet and the outlet. When the steady conditions of the target discharge are achieved, the model automatically steps to the next discharge. The hydrodynamic conditions at the end of a step are used as initial conditions for the next step. Thus, this option uses the time strictly necessary to reach the steady flow conditions of any of the constant discharges defined by the user, without having to know the time to reach the steady flow conditions for any discharge and reducing the computational time to a minimum.

2.3. CUDA Fortran code: R-Iber

The sequential version of Iber is partially parallelised by means of the open multi-processing (OpenMP) technique. However, the intrinsic limitations of this technique only allow for speed-ups corresponding to the number of CPU cores, at most. Despite the computing time of the hydrodynamics being reduced notably, the simulation of long stretches of rivers, even entire rivers, or long time series for fish habitat assessment procedures remains unapproachable with techniques based solely on CPU computing.

The integration of several calculation modules in the Fortran-based code of Iber was originally functionality-oriented, prioritising the full integration of all modules instead of multi-core processing efficiency. Due to the growing application of more complex and detailed simulations in river hydrodynamics demands an increase in computational capacity and, thus, a code re-ordering and optimization was already made in previous versions of Iber. Despite that, the simulation of models of thousands or millions of elements, or long-time series, requires several hours or even days of computational time with the sequential version.

R-Iber is a new code that implements a GPU parallelisation of the hydrodynamic (Bladé et al., 2014b) and habitat (Sanz-Ramos et al., 2019) modules of Iber based on CUDA Fortran architecture. An efficient CUDA programming requires not only a hierarchical organisation of the computing units but also the programming of each thread block to efficiently process data in parallel (Zhang and Jia, 2013). To achieve this, the original code of Iber was re-organised and re-written to follow the main structure of CUDA programming, that is: transfer data from CPU memory (host) to GPU memory (device); run parallel computing through 'kernels'; and transfer data back to the host from the device. More details of the structure of the code are described in Appendix A.

The main limitation of GPU-parallelised codes is the memory access and, especially, the memory transfer (García-Feal et al., 2018; Vacondio et al., 2014; Zhang and Jia, 2013). R-Iber reads, transfers and writes memory data only when it is strictly necessary, with the aim of maximising the code's efficiency. Another issue, which also occurs in CPU computing, is that of the multi-core computing simulations: running several simulations at the same time in the same processor unit creates a significant bottleneck, particularly for GPU computing, and reduces the global computing capacity of the device (Morales-Hernández et al., 2021). To minimise heavy performance penalties, R-Iber allows for the selection of the GPU device on which to carry out each calculation. Thus, the option of a multi-processor computation on a single computer with several GPUs or on a cluster of GPUs is available to practitioners. Fig. 1 presents the main workflow of the R-Iber code.

Additionally, to achieve maximum performance on GPU processors on arithmetic operations, it is necessary to use as many single-precision

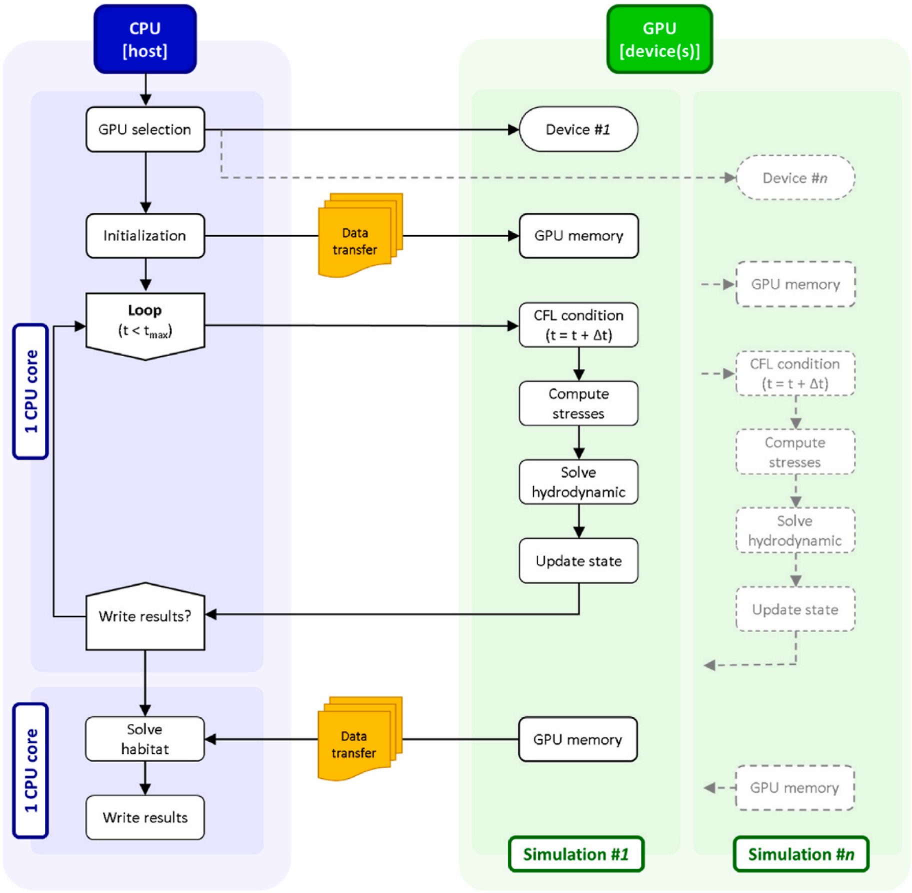

Fig. 1. General flow chart of the R-Iber code for a particular GPU computation. The sketch also presents the flow for n simulations on n different devices.

arithmetic operations as possible (Hwu et al., 2009), as it is done in R-Iber. Using single-precision operations implies round-off errors in the calculation results, i.e. after a single floating-point operation the result is rounded after the seventh digit. However, CPU-based simulations perform double-precision arithmetic operations, as it is done in Iber, with similar performance to single-precision (Narumi et al., 2011).

On the other hand, the habitat module of Iber, and also of R-Iber, is computed as a post-process because the currently implemented fish suitability curves only depend on the hydrodynamics. Thus, for optimum memory access/transfer, the information exchanged between hydrodynamics and habitat must be done directly in the host and only when the results have to be written. This moment may occur when the simulation time is greater than the user-defined time to write the results, or when the steady flow conditions are accomplished if the 'stepped discharge' option is used. Additionally, the process of writing the results utilises an independent CPU core (Fig. 1). Therefore, once all data is transferred back to the host, the habitat module is computed in the CPU while the GPU continues calculating without any performance penalty.

It is worth noting that 2D-SWE-based models do not solve the energy equation, which in 1D only depends on the energy balance between two consecutive sections. In 2D models, a steady state is reached when the inlet discharge is equal to the outlet discharge and, thus, the whole flood front propagation process must be solved anyway. This implies an increase in the computational time because the simulation time needed to reach steady conditions in general is unknown. Therefore, longer simulation times are required to ensure a steady-state.

This particular issue is solved with a specific option called 'stepped discharge', which allows for the simulation of steady flow conditions for several discharges in the same model and directly provides flow-habitat relationships such as the WUA. With this option enabled, GPU parallel computation would potentially reach its maximum calculation capacity as the results would only be written a few times (at each step).

2.4. Hardware and characteristics

Simulations were carried out with Iber v3.1, which contains the new code of R-Iber and are freely distributed through www.iberaula.com. Both algorithms use the Roe 1st order numerical scheme. Computations with the sequential version (CPU) were done with a CPU Intel Core i7-9750H, while computations on the CUDA Fortran GPU version (R-Iber) were launch with the same CPU but computed in different GPU devices (Table 1). The NVIDIA GPUs selected were the GeForce® GTX and RTX series which, being quite common devices for standard desktop computers and mid-range to high-end gaming laptops, cover a wide temporal range.

3. Validation

3.1. Test 1: flooding of disconnected floodplains

The first validation test was the so-called 'Test 1' proposed by the United Kingdom Environment Agency within the Defra Flood and Coastal Erosion Risk Management Research and Development Programme (Néelz and Pender, 2013). This test aims to assess the capability of the 2D hydrodynamic models to reproduce the flooding of disconnected floodplains and the wetting and drying processes.

The domain consisted of a 700 × 100 m channel with a bottom elevation composed of an increasing slope (≈0.02%), followed by a decreasing slope (≈0.25%), and ending in an increasing slope (≈0.3%). Thus, a depressed area was generated, where the water would be retained. As boundary condition, a water level was imposed, varying from 9.7 to 10.35 m in 1 h, keeping a constant value for 8 h to ensure the depressed area was completely filled, then returning to 9.7 m in 1 h.

Table 1
Graphical power units (GPU) utilized in the computations.

Model	Release date	Architecture	Cores	Memory (type)
GeForce GTX 980 Ti	02/06/2015	Maxwell	2816	6 GB (GDDR5)
GeForce GTX 1660 Ti[a]	22/02/2019	Turing	1536	6 GB (GDDR6)
GeForce RTX 3070[a]	29/10/2020	Ampere	5120	8 GB (GDDR6)

[a] *This GPU is built for laptop.*

Two calculation scenarios were performed: one following the proposed domain discretisation, with 1125 mesh elements, and the other using the full digital elevation model (DEM) resolution, which provides 26,341 calculation points. Simulations were also done with the CUDA C++ GPU code of Iber, called Iber+ (García-Feal et al., 2018).

Fig. 2 shows the water evolution at the two control points: P1 (400,50) and P2 (600,50). The three numerical models show the same hydraulic behaviour: water accumulated in the depressed area at an elevation of 10.25 m, flush with the topography.

The computational times of the reference model (Iber v3.1 sequential) were 44 and 2064 s for the proposed discretisation and the full DEM models, respectively. The speed-ups of R-Iber reached 3.4 and 39.4-times, while Iber + reached 2.8 and 40.5-times, respectively, for the GTX 1660 Ti. Similar values were obtained for the GTX 980 Ti and the RTX 3070 devices (Table 2).

It is worth noting that for the proposed discretisation, in which only 1125 elements were used, the speed-up was not significant because the parallelised part of the code was faster than the time required to transfer information from the device to the host and to write the results file. This bottleneck is practically neglected when the number of elements increases.

3.2. Test 2: Hydraulic jumps and flow obstructions

The second validation case is the 'Test 6A' of Defra's benchmark (Néelz and Pender, 2013). This case aims to verify the capability of 2D-SWE-based models to simulate transcritical flow regimes, hydraulic jumps and wakes behind obstructions. For that purpose, the experiment of Soares-Frazão and Zech (2007) was simulated in Iber and R-Iber using two different mesh discretisation of rectangular elements: that proposed by Defra's benchmark (56,616 elements) and the full DEM resolution (226,352 elements).

An initial water elevation of 0.4 m was imposed from the beginning of the flume to the narrowing of it, upstream of the obstacle. This configuration tries to reproduce a dam-break process in the downstream area, where the obstacle is placed non-symmetrically on a wet area in the flume. Results were extracted each 0.1 s, considering a fixed time step of 0.005 s. Six control points monitored the water depth and velocity during the experiment (G1 to G6).

All numerical approaches behaved similarly. Fig. 3 shows the evolution of the water depth and velocity at points G1, G2 and G3. The arrival time of the flood front was the same and suitably captured both the supercritical and subcritical flow regimes. At point G2, the presence of the obstacle generated a mobile hydraulic jump upstream at around 12 s, where water depth evolved from 0.03 to 0.1 m during the 10 s after the shock wave. In the case of the proposed mesh discretisation, the hydraulic jump was produced at 9.4 s (yellow and grey dashed line), while with the full DEM the hydraulic jump was produced at 16.3 s for Iber (black dashed line) and 11 s for R-Iber (red line). Iber generated a weak hydraulic jump at 11 s, which then transformed into a strong hydraulic jump a few seconds later (16.3 s). This difference, in this particular case of the simulation of a hydraulic jump with a very fine discretisation of the calculation domain (grid of 0.05 × 0.05 m), can be attributed to the fact that R-Iber computes in single precision, while Iber does it in double precision. Thus, after a single floating-point operation the result is rounded after the seventh digit in R-Iber.

In general, the reproduction of a hydraulic jump is quite complex to reach with full precision, particularly in 2D-SWE-based modelling when the hydraulic jump evolves along time due to the discharge is not constant. A sharper solution is generally obtained (Néelz and Pender, 2013).

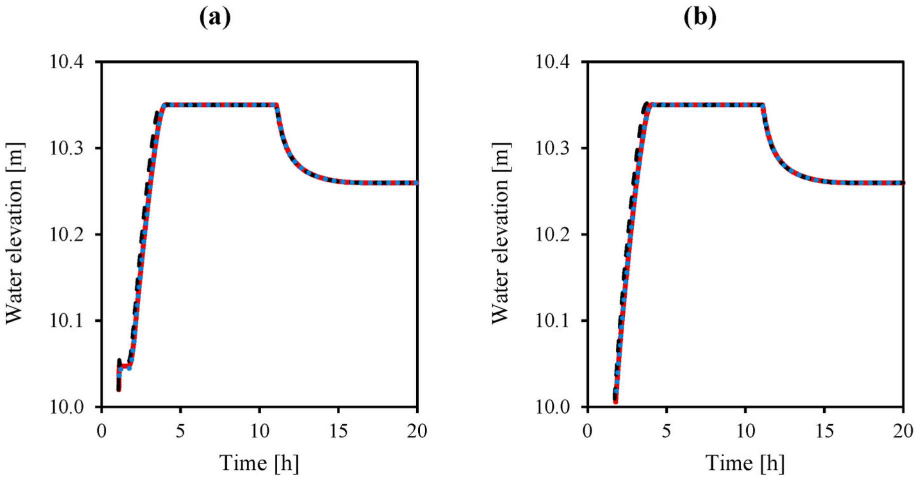

Fig. 2. Evolution of the water elevation at control points P1 (a) and P2 (b) for Iber (black dashed-line), Iber+ (blue dotted-line) and R-Iber (red line).

Table 2
Computational time, in seconds, of the Test 1 for the sequential (Iber) and paralelized (R-Iber) versions. The speed-up is the quotien between parallelised and sequential computational times.

Model	Sequential [s]		Parallelised [s]		Speed-up [-]	
	1125 els.	26,341 els.	1125 els.	26,341 els.	1125 els.	26,341 els.
GeForce GTX 980 Ti	44	2064	13	61	3.4	33.6
GeForce GTX 1660 Ti			13	52	3.4	39.4
GeForce RTX 3070			10	57	4.4	41.1

Despite that, the flow patterns were well captured by R-Iber, even using single precision and a Roe 1st order numerical scheme (Cea et al., 2010).

The numerical simulation in the sequential code (Iber) spanned 172 s for the proposed discretisation and 706 s for the full DEM model, while the parallelised R-Iber code computed the models in 35–45 s and from 130 to 197 s, respectively. This means an average speed-up of around 3.6–5.4 times with respect of the sequential code (Table 3). It is worth noting that the necessity of writing results at very small-time steps (0.1 s) considerably reduces the global simulation time. If only computational time is considered, depending on the GPU used, the speed-up of R-Iber reaches values from 65.4 to 75.3 and from 96.8 to 140.4-times for the proposed and full DEM models, respectively (Table 3, values in brackets).

3.3. *Test 3: fishway and recirculation areas*

Test 3 is the numerical reproduction of the laboratory experiment presented by Puertas et al. (2004), which consisted of the hydraulic characterisation of a vertical slot fishway. The original flume device was a 12 m long channel divided into 11 pools (four for the design of Test 1 and four for the Test 2 design, while the rest were the upper, intermediate, and lower pools). Pool #7, which belonged to the Test 1 design (Fig. 4a), was analysed considering half of the flume, a 5.7% slope and a discharge of 0.0741 m^3/s. A detailed description of the flume experiments can be found in Puertas et al. (2004).

Previous numerical experiments confirm the capability of 2D-SWE-based models for modelling the free surface flow in vertical slot fishways (Bermúdez et al., 2010; Cea et al., 2007; Puertas et al., 2012). Thus, this validation case aimed to reproduce main (jet) and particular (recirculation areas) flow patterns (Fig. 4b) by considering four mesh discretisation: 2751 (M1), 5502 (M2), 22,008 (M3) and 88,032 (M4) elements. In general, a mesh size reduction implies a better representation of the hydrodynamics and, consequently, the eco-hydraulic assessment. However, higher computational times are required.

The numerical discretisation of 2751 elements (M1) provided smooth results, with only a weak recirculation area on the right side downstream of the pool inlet and a considerably straight main jet (Fig. 5a). This recirculation area increased as the number of elements doubled (M2), and another two weak eddies appeared on the upstream and downstream corners on the left side, between the baffle and the wall (Fig. 5b). A computational mesh of eight times more elements (M3) than the first mesh (M1) allowed for the proper definition of two separately recirculation areas on both sides of the main jet (Fig. 5c). This domain discretisation effectively defined the general flow pattern shown in Fig. 4b, with a well-defined main jet. In the model with a mesh of 88,032 elements (M4), the flow patterns became more complex, representing small eddies near the bigger eddies to both sides of the main jet (Fig. 5d).

Numerical results were compared to the experimental results throughout the mean depth of the middle traverse section (h_0), the mean flow depth of the pool (h_m), the maximum depth of the pool (h_{max}), the minimum depth of the pool (h_{min}), the depth of the slot (h_s), the absolute velocity of the slot ($|v_s|$), the discharge coefficient of the slot ($C_d = Q/(bh_s v_s)$, where b is the slot width) and the energy dissipation rate in the pool ($E_d = (\rho g Q S_0)/(B h_0)$, where ρ is the flow density, g is the gravitational acceleration, Q is the flow discharge, S_0 is the bottom slope and B is the pool width). Table 4 summarises the experimental and numerical results obtained with each numerical mesh.

In general, R-Iber performed suitably for all the simulations, particularly for the finer meshes (Table 5), which provided a good fit for the observations reproducing the flow patterns, such as eddies and the shape and dimension of the main jet. The M1 mesh (2751 elements) showed the poorest results, with absolute relative errors slightly above 10% in some hydraulic parameters (h_0, h_m and E_d). By contrast, the M3 and M4 meshes (22,008 and 88,032 elements, respectively), provided suitable results with errors below 3.5%. Numerical results of the discharge coefficient (C_d) and the energy dissipation rate (E_d) also adjusted suitably to the observations, with a relative error less than 3.5% for M3 and M4 meshes.

The benefit of using the CUDA Fortran GPU parallelisation R-Iber instead of Iber is the considerable reduction in computational time (Table 6). In this particular case, R-Iber reached a speed-up from 23.9 (GTX 980 Ti) to 45.1-times (RTX 3070) for mesh M4 in comparison with the sequential version. Additionally, the efficiency of the code can be evaluated by accounting for the computational cost per number of elements. The computational time required by Iber increased from 24.7 (M1) to 106.6 s (M4) per 1000 elements, while in the case of R-Iber, it decreased from 5 to 2.9 s. Thus, it can be seen that the new parallelised

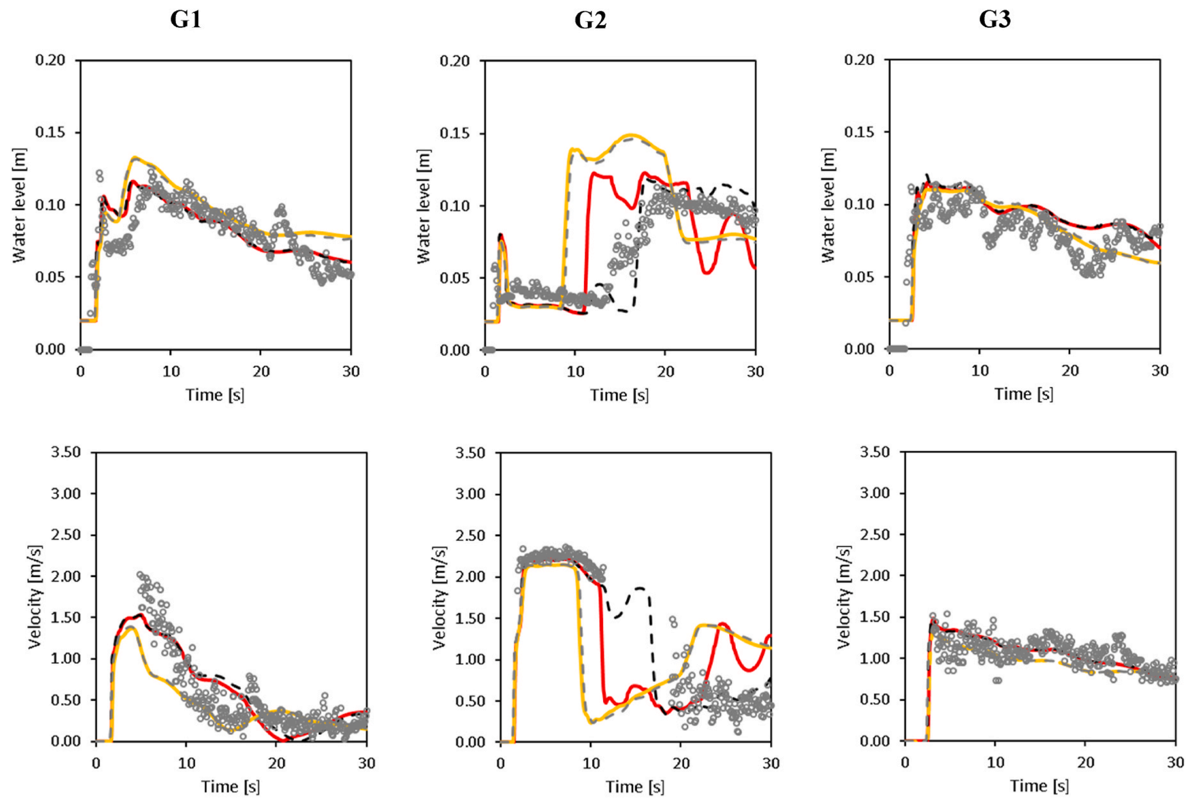

Fig. 3. Evolution of the water depth (up) and velocity (down) at control points G1, G2, and G3. Grey circles: experimental data; Dashed lines: Iber for the proposed discretisation (grey) and the full DEM (black); Continuous lines: R-Iber for the proposed discretisation (yellow) and the full DEM (red).

Table 3
Computational time, in seconds, of the Test 2 for the sequential (Iber) and paralelized (R-Iber) versions. The speed-up is the quotien between parallelised and sequential computational times.

Model	Sequential [s]		Parallelised[a] [s]		Speed-up[a] [-]	
	56,616 els.	226,352 els.	56,616 els.	226,352 els.	56,616 els.	226,352 els.
GeForce GTX 980 Ti	172	706	45 (3)	197 s (7)	3.8 (65.4)	3.6 (96.8)
GeForce GTX 1660 Ti			42 (2)	158 s (6)	4.1 (70.8)	4.5 (110.1)
GeForce RTX 3070			35 (2)	130 s (5)	4.9 (75.3)	5.4 (140.4)

[a] *Net computational time, without the time required to write the results (in brackets).*

code of Iber, R-Iber, provides not only a valuable computational cost reduction but also a notable improvement in the efficiency of the computations when the number of elements of the model increases.

4. Study cases

The performance of the model has been tested in two real study cases: Eume River and Cinca River (Fig. 6). The Eume case study is focused on showing the benefits of using not only the GPU-parallelised eco-hydraulic model of Iber, R-Iber, but also the noticeable improvement of using the 'stepped discharge' inlet condition instead of creating a separate model for each discharge.

An intrinsic benefit of the GPU parallelisation of 2D-SWE-based models is the capability to assess long-term hydrodynamics in long-rivers in a reasonable timeframe. If a fish habitat module is integrated into the code, such as in R-Iber, the eco-hydraulic evaluation of rivers will no longer be limited to a few metres or short river stretches. To demonstrate this, the capacity of R-Iber to simulate long-term fish suitability variations in long-river stretches (even entire rivers) is

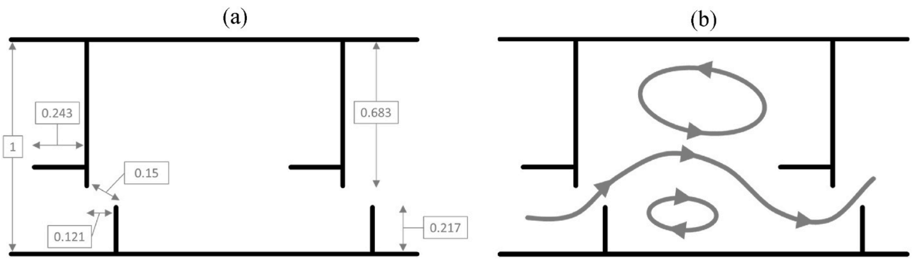

Fig. 4. (a) Geometry of the Test 1 design pool (distances in meters). (b) General flow pattern in Test 1 design pool (sketch adapted from Puertas et al. (2004)).

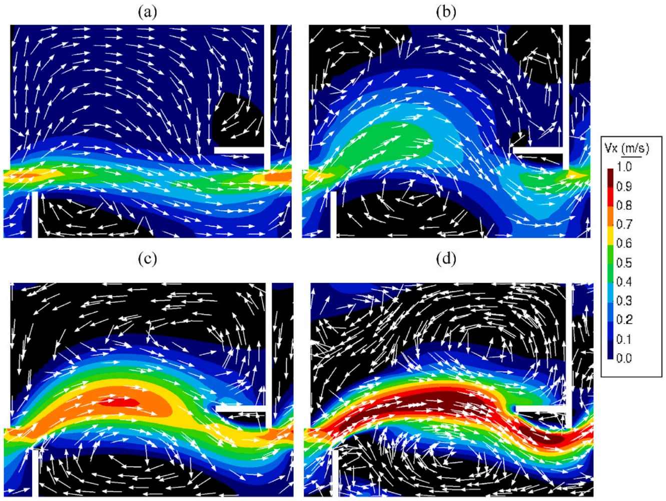

Fig. 5. Numerical results of the depth-averaged velocity vectors (white rows) and contour map (colored) in the *x* direction (negative velocities are plotted in black). Mesh of 2751 (a), 5502 (b), 22,008 (c) and 88,032 (d) elements.

presented in the case study of the Cinca River.

4.1. Improved IFIM for 2D-SWE-based models: Eume River

The analysed stretch of the Eume River, located in the north west of Spain (Fig. 6a), is characterised by two well-differentiated geomorphological facies: a discontinuous channel with jumps and pools upstream and a continuous channel downstream. All discharges were evaluated with Iber and R-Iber considering a separate model for each discharge and also using the 'stepped discharge' option, which consisted of a unique model. In this case, the tolerance was fixed at 1%: a new 'step' of the series of inlet discharges was automatically imposed when the absolute value of the outlet discharge minus the inlet discharge, all divided by the inlet discharge, was less than the tolerance.

The study area of 3 km in length (Fig. 6b) was discretised into 72,426 calculation elements. Twelve discharges were evaluated, ranging from 0.149 to 11.770 m^3/s. *Salmo trutta* was the target specie, and the depth- and velocity-dependent suitability curves described in CHE and ACA, (2008) were used as biological information. A detailed description of the study area can be found in Sanz-Ramos et al. (2019).

As expected, the WUA depended on the hydrodynamics of each evaluated flowing discharge. Fig. 7 shows, in the transition zone between two geomorphological facies (Fig. 6b, hollow black square), the elemental suitability evaluated for different discharges and the adult stadium (product of the depth- and velocity-suitability). Low discharges produced a narrow-wet area, particularly at the facies characterised by jumps and pools (Fig. 7a and b). The most fish suitability was obtained in zones with high depths (pools). When the discharge increased (Fig. 7c), the discontinuous channel became continuous, the velocity increased, and the suitability of this area decreased. This is clearly seen in the lower part of the river, where a moderate depth and low velocity area provided a high suitability zone. However, high discharges (11.77 m^3/s) modified the hydrodynamics in this area, reducing the suitability of the central part of the channel and displacing it to the lateral sides (Fig. 7d). The resulting WUA is reduced for all flows and stadiums of the target specie, remaining below 14% of the total wetted area. The maximum suitability conditions were achieved in the fry for a discharge of 0.560 m^3/s (12.78% of the wetted area) and in the juvenile and adult stadium for 2.176 m^3/s (fry, 8.8%; adult, 6.2% of the wetted area).

Identical hydrodynamic and habitat results were obtained with Iber and R-Iber, but with significant differences in the computational time (Table 7). The simulation process of computing each discharge per model required between 195 and 357 s in the sequential mode (CPU), while the GPU version required less than 30 s for each simulation (Fig. 8a). Accounting for the total computational time of all the models, a global time of 2844 s was necessary for the CPU version. This time was reduced to 207 s for the GTX 980 Ti, 189 s for the GTX 1600 Ti, and 124 s for the RTX 3070 (Fig. 8a).

The benefits of using the 'stepped discharge' option instead of a separate model for each discharge was evaluated as the quotient between the addition of the time of each model and the time of the model that used the 'stepped discharge' option. The advantage of using the 'stepped discharge' option instead of a separate model for each discharge is proved by a 16.6% acceleration in the computation time in CPU-based simulations (Fig. 8b). When GPU calculations were applied, speed-ups of 32–52% were achieved (Fig. 8b). Using the RTX 3070 GPU did not reduce the computation time as much as possible due to the model's low number of elements. However, when a higher number of elements discretise the domain, the advantage of using a more powerful GPU clearly shows its potentialities (as shown in section 4.2).

It is worth noting that only the computation time was considered in the previous comparison: the time needed for changing the boundary condition was not taken into consideration. If a constant time of 30 s for each simulated discharge is considered as the necessary time for changing the boundary conditions and re-starting the simulation, a global speed-up of around 350% would be reached for the GPU computations of the 'stepped discharge' option.

4.2. Long-term simulations in long-rivers stretches: Cinca River

Cinca is a 191 km long mountain river that begins in the central part of the south of the Pyrenees and drains into the Ebro River, in Spain (Fig. 6a). The analysed stretch of the Cinca River is 11 km long, starting 2.5 km upstream of the Bellós River junction and ending at the Ara River junction (Fig. 6c). This stretch is characterised as a braided river with a considerably active morphology (Béjar et al., 2018; Vericat et al., 2017).

The flood event of 9 October 2014, which had two peak discharges and spanned 10 days (CHE, 2021), was simulated with three different meshes of 74k elements (M1), 299k elements (M2), and 1885k elements (M3). The river domain was discretised using an irregular mesh of

Table 5
Relative error (in absolute value) of the numerical results for T1 design, 5.7% slope, and Q = 0.0741 m^3/s.

	h_0 [%]	h_m [%]	h_{max} [%]	h_{min} [%]	h_b [%]	$\lvert v_0\rvert$ [%]	C_d [%]	E_d [%]
M1	11.7	10.2	7.4	8.3	8.4	9.7	2.3	10.5
M2	7.1	5.6	3.9	2.1	4.1	8.9	5.7	6.7
M3	3.5	2.4	2.3	1.0	2.6	4.4	2.1	3.4
M4	2.7	2.0	3.4	2.6	3.3	3.1	0.1	2.7

Table 4
Experimental and numerical results for the Test 1 design, 5.7% slope and Q = 0.0741 m^3/s.

	h_0 [m]	h_m [m]	h_{max} [m]	h_{min} [m]	h_s [m]	$\lvert v_s\rvert$ [m/s]	C_d	E_d [W/m^2]
Exp.	0.604	0.608	0.652	0.562	0.604	0.880	0.870	69.350
M1	0.675	0.670	0.700	0.608	0.655	0.795	0.890	62.040
M2	0.647	0.642	0.677	0.574	0.629	0.801	0.919	64.675
M3	0.625	0.622	0.667	0.568	0.620	0.841	0.888	66.980
M4	0.620	0.620	0.674	0.577	0.624	0.852	0.871	67.490

Table 6
Computational time, in seconds, of the Test 3 for the sequential (Iber) and paralelized (R-Iber) versions. The speed-up is the quotien between parallelised and sequential computational times.

Model	Sequential [s]				Parallelised [s]				Speed-up [-]			
	M1	M2	M3	M4	M1	M2	M3	M4	M1	M2	M3	M4
GeForce GTX 980 Ti	68	136	1138	9387	22	26	94	392	3.1	5.2	12.1	23.9
GeForce GTX 1660 Ti					14	18	55	257	4.9	7.6	20.7	36.5
GeForce RTX 3070					13	15	47	208	5.2	9.1	24.2	45.1

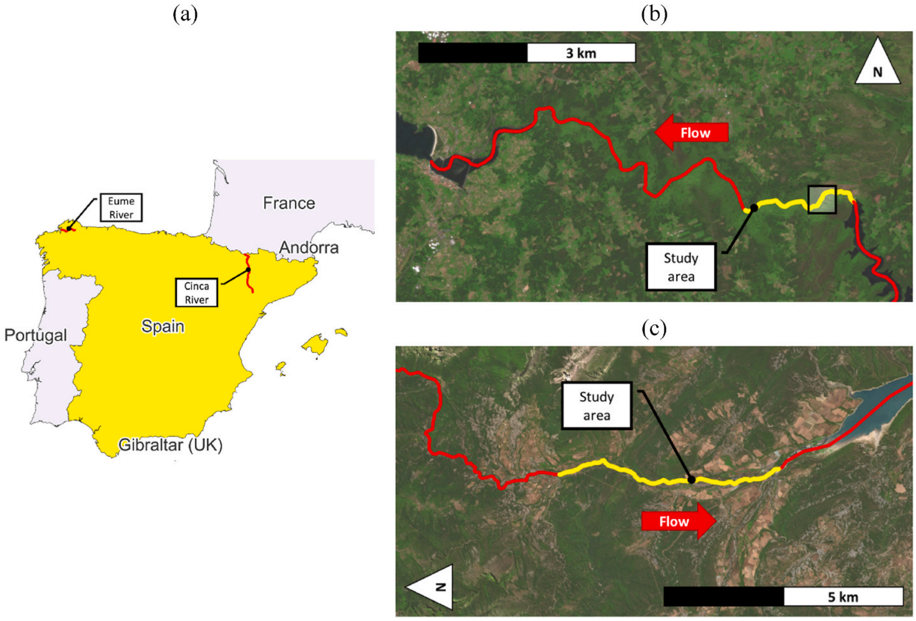

Fig. 6. (a) General location of Eume and Cinca rivers (red lines). (b) Study area of the Eume River (yellow line) and the location of the results shown in Fig. 7 (hollow black square). (c) Study area of the Cinca River (yellow line).

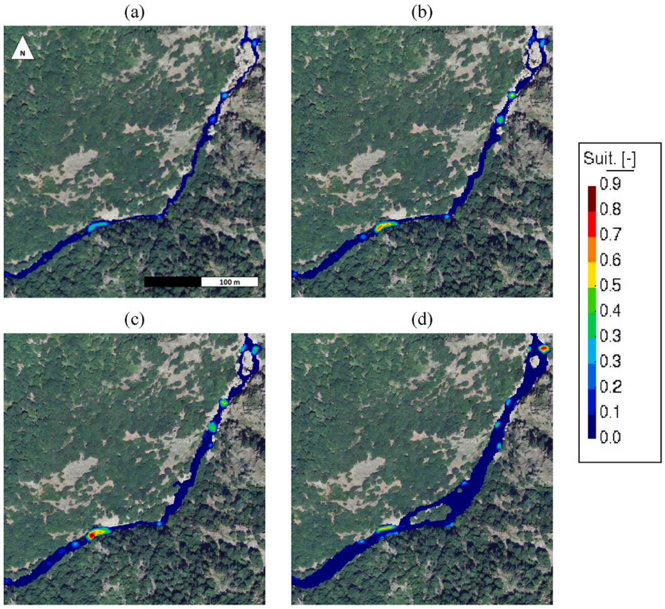

Fig. 7. Hydraulic suitability at the stream analysed for the adult stadium of *Salmo trutta* according to the suitability curves of Bovee (1982): (a) 0.149 m^3/s, (b) 0.560 m^3/s, (c) 1.567 m^3/s, and (d) 11.77 m^3/s (background image: IGN (2021)).

triangular elements with 220 (M1), 887 (M2) and 5577 (M3) elements per hectare, the last one being one order of magnitude above the common values used in flood studies (Sanz-Ramos et al., 2020a). The mesh was updated with the 2 × 2 m DEM provided by National Geographic Institute of Spain (IGN, 2022). During these 10 days, where discharges ranged from 10 (base flow) to 250 m^3/s (maximum peak discharge), variations in the fish habitat suitability were evaluated for salmonids, *Salmo trutta* (CHE and ACA, 2008), and cyprinids, *Chondrostoma polylepis* and *Barbus bocagei* (Martinez, 2000). These target species were selected within the Cinca's basin characteristics (CHE, 2002).

In contrast with the IFIM, the main result of this analysis is the evolution of the WUA over time, besides the evolution of the fish suitability distribution. Fig. 9a presents the evolution of the WUA (in %) for the three abovementioned species and stadiums (fry, juvenile, and adult) and the M2 domain discretisation. Changes in the hydrological regime also modify the WUA. As expected, low discharges favoured a more suitable area for fry and juvenile stadiums. Despite high discharges generating high depths and velocities, in general, other areas flooded

Table 7
Computational time, in seconds, of the Study Case 1 for the sequential (Iber) and paralelized (R-Iber) versions. The speed-up is the quotien between parallelised and sequential computational times.

Model	Sequential [s]	Parallelised [s]	Speed-up [-]
	72,426 els.	72,426 els.	72,426 els.
GeForce GTX 980 Ti	2844 s	207 s	13.7
GeForce GTX 1660 Ti		189 s	15.0
GeForce RTX 3070		124 s	23.0

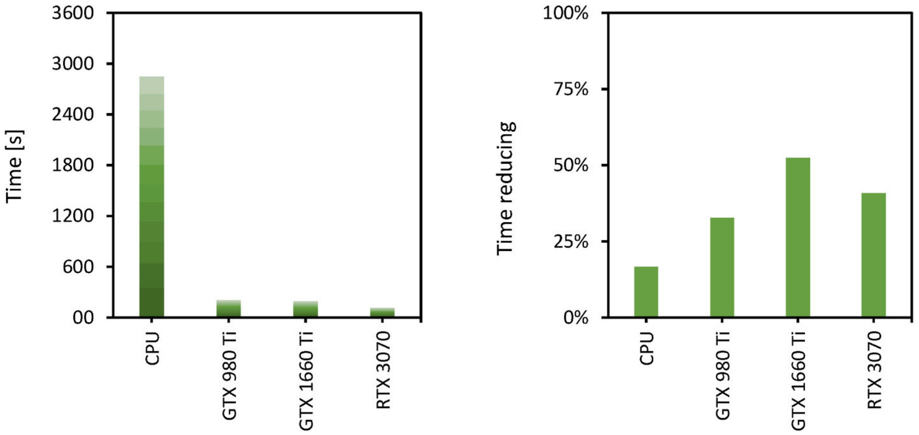

Fig. 8. (a) Simulation time of each discharge computed independently (low discharges: dark green; high discharges: light green). (b) Time reducing obtained when the 'stepped discharge' option is applied in comparison to the independent computing of each discharge.

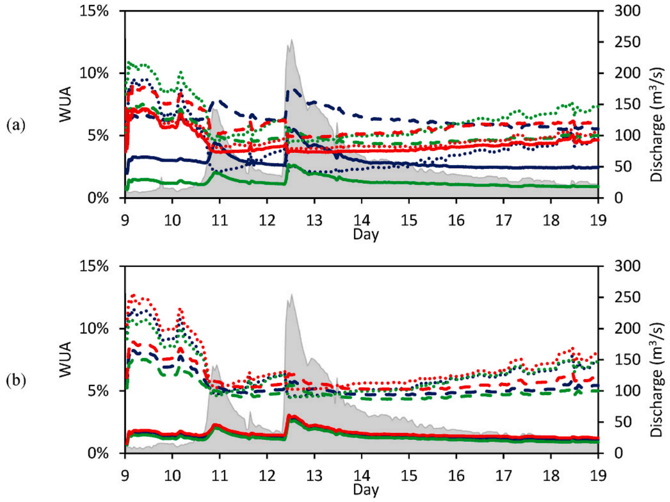

Fig. 9. (a) Evolution of the weight useable area (WUA) during the event of 9 October 2014 for adult (continuous line), juvenile (dashed-line) and fry (dotted-line) stadiums of *Chondrostoma polylepis* (black), *Barbus bocagei* (green) and *Salmo trutta* (red) (mesh M2). (b) Sensibility analysis of WUA for the stadiums of *Barbus bocagei* (continuous line: adult; dashed line: juvenile; dotted line: fry) considering different mesh discretisation: M1 (black), M2 (green) and M3 (red). The grey area represents the hydrograph.

provided more suitable zones for the *Chondrostoma polylepis* (black lines) and *Barbus bocagei* (green lines), while the WUA of the *Salmo trutta* (red lines) decreased.

Fig. 9b exemplifies the variation in the WUA evolution for adult (continuous line), juvenile (dashed line) and fry (dotted line) of the species *Barbus bocagei* when the models of 220 (M1, black line), 887 (M2, green line) and 5577 (M3, red line) elements per hectare were considered. As has also been demonstrated in sections 3.2 and 3.3, a finer discretisation of the study area provides hydrodynamic results of a higher resolution, which are the bases of WUA assessment. In general, the M2 mesh provided a mean increment of 7.9% of the WUA in comparison to the M1 mesh, while the M3 mesh reached up to 18.1% more WUA than the M1 mesh.

In terms of computational time, the sequential code (Iber) required 7.4 h for the mesh M1, 71.3 h (≈3 days) for the mesh M2, and 1081.3 h (≈45 days) for the mesh M3. For the M1, M2 and M3 mesh configurations, R-Iber reached speed-ups from 19.8 to 183.1-times, respectively (Table 8).

The efficiency of the code can be evaluated by the computation time required per 1000 elements. The time required by Iber increased when the number of elements increased from 356 to 2062 s, while in the case of R-Iber, the time remained almost constant, at around 10–20 s per 1000 elements. A similar trend was obtained in the validation tests.

Complementary to the traditionally used IFIM, the assessment of the fish habitat suitability considering real discharge scenarios –even in real time– can be a step forward in eco-hydraulics as it is not limited to steady conditions (particular constant discharges). Furthermore, it also encourages the study of the convenience, or inconvenience, of reintroducing native species and the potential prevalence of invasive species to the natural or induced hydrologic regime of a river. Additionally, since hydrodynamic conditions in rivers vary over time due to morphodynamic changes, if sediment transport (Hung et al., 2022; Pisaturo et al., 2021) and water quality (Wang and Lin, 2013) processes are considered, this kind of modelling strategy would allow for the analysis of such conditions from a holistic point of view.

5. Conclusions

Currently, eco-hydraulic numerical tools are widely used for river habitat rehabilitation, restoration and enhancement purposes. These tools undergo continuous development due to the advances in data-acquisition and data-treatment and the use of high-performance techniques to formulate more efficient, robust, and powerful numerical codes. Nevertheless, 2D-SWE-based eco-hydraulic numerical tools that include an integrated GPU-parallelised hydrodynamic module and

Table 8
Computational time, in hours, of the Study Case 1 for the sequential (Iber) and paralelized (R-Iber) versions. The speed-up is the quotien between parallelised and sequential computational times.

Model	Sequential [h]			Parallelised [h]			Speed-up [-]		
	M1	M2	M3	M1	M2	M3	M1	M2	M3
GeForce GTX 980 Ti	7.4	71.3	1080	0.4	1.6	16.2	19.8	45.0	66.8
GeForce GTX 1660 Ti				0.3	1.1	11.6	26.6	64.3	92.8
GeForce RTX 3070				0.2	0.6	5.9	37.2	116.8	183.1

physical habitat module developed for overcoming the main computational limitations are lacking.

R-Iber is a GPU parallelised hydrodynamic numerical tool that integrates a physical habitat module; thus, it is a fully-integrated GPU-parallelised eco-hydraulic tool. The code, based on Iber, was developed in CUDA Fortran language for faster computations. The hydrodynamic module of R-Iber was first validated using two benchmark test cases and a laboratory experiment with a fishway. R-Iber was also applied to two real cases, one following the IFIM and the other simulating a 10-day real flood event.

The benefit of using a GPU-parallelisation eco-hydraulic tool instead of a CPU-based tool is the significant reduction in computation time, with speed-ups of one or two orders of magnitude (above 100-times with respect CPU computations), but also a notable improvement in the efficiency of the computations when the model's number of elements increases is shown. Additionally, the option 'stepped discharge' demonstrated to be a suitable solution to address Q-WUA computations following the IFIM, being the computations 50% faster than an in-cascade simulation process. This option uses the time strictly necessary to reach the steady flow conditions without having to know the time to reach the steady flow conditions for any discharge and reducing the computational time to a minimum.

R-Iber can simulate calculation domains discretised with finer calculation meshes providing high-resolution numerical models with a better representation of the hydrodynamics and, consequently, the habitat, with no performance penalties. Additionally, it has been proven that the simulation of long river stretches, even entire rivers, or long-term habitat analysis can be computed with GPU-based numerical codes within a convenient timeframe.

Funding

The contract of the D.D.-S. is funded by the International Center for Numerical Methods in Engineering (VAC-2021-1).

Declaration of competing interest

The authors declare the following financial interests/personal relationships which may be considered as potential competing interests: Danial Dehghan Souraki reports financial support was provided by Centre Internacional de Mètodes Numèrics en la Enginyeria.

Data availability

The authors do not have permission to share data.

Appendix A. CUDA Fortran structure of R-Iber

This appendix shows the internal structure of the new code R-Iber, which is based on CUDA Fortran programming language (NVIDIA, 2022b). The main structure of the code R-Iber is depicted in Fig. 1 of the main manuscript.

R-Iber code can be split in two main parts: the host and the device. The host relates to the central processing unit, or CPU, and controls the main instructions of the code (variable reading, allocatation, saving, transfer, etc.) and directives (e.g. loops), even the execution of the graphics processing unit, or GPU. This last action is done through Kernel Loop Directive (KLD).

The host part of code of R-Iber can be synthetized as follow.

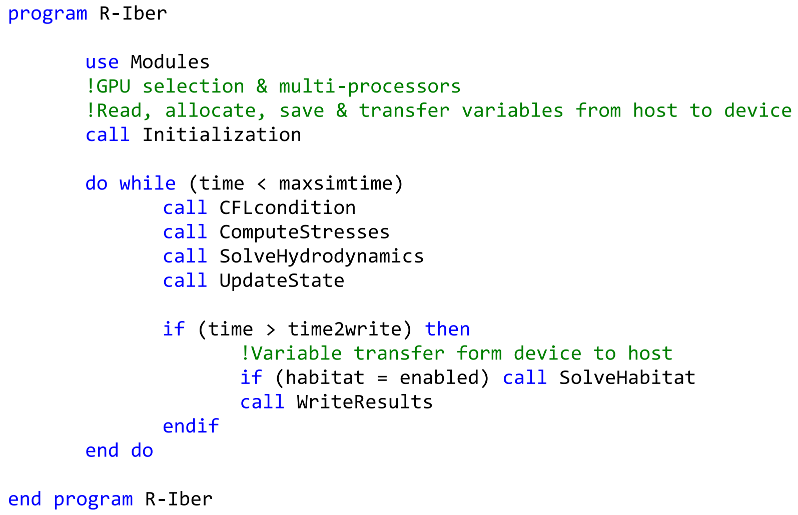

```
program R-Iber

       use Modules
       !GPU selection & multi-processors
       !Read, allocate, save & transfer variables from host to device
       call Initialization

       do while (time < maxsimtime)
              call CFLcondition
              call ComputeStresses
              call SolveHydrodynamics
              call UpdateState

              if (time > time2write) then
                     !Variable transfer form device to host
                     if (habitat = enabled) call SolveHabitat
                     call WriteResults
              endif
       end do

end program R-Iber
```

Loops of the original code of Iber have been adapted to the new structure of the CUDA Fortran programming and both codes, Fortran and CUDA Fortran, can be called from the host as follows.

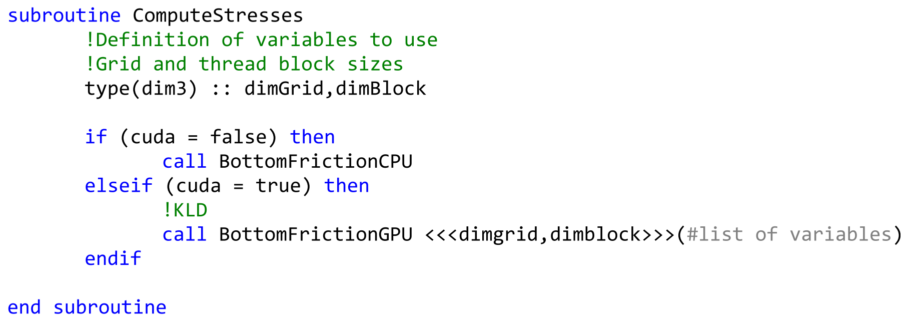

```
subroutine ComputeStresses
       !Definition of variables to use
       !Grid and thread block sizes
       type(dim3) :: dimGrid,dimBlock

       if (cuda = false) then
              call BottomFrictionCPU
       elseif (cuda = true) then
              !KLD
              call BottomFrictionGPU <<<dimgrid,dimblock>>>(#list of variables)
       endif

end subroutine
```

A kernel may be invoked with many thread blocks, each with the same thread block size. The thread blocks are organized into a one-, two-, or three-dimensional grid of blocks, so each thread has a thread index within the block, and a block index within the grid (Zhang and Jia, 2013). When invoking a kernel, the first argument in the chevron <<<>>> syntax is the grid size, and the second argument is the thread block size. Thread blocks must be able to execute independently; two thread blocks may be executed in parallel or one after the other, by the same core or by different cores.

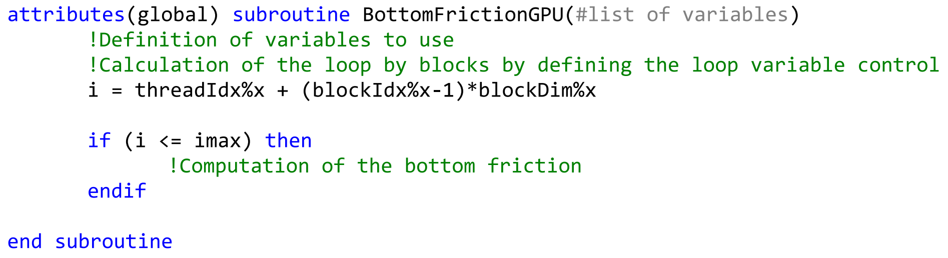

```
attributes(global) subroutine BottomFrictionGPU(#list of variables)
       !Definition of variables to use
       !Calculation of the loop by blocks by defining the loop variable control
       i = threadIdx%x + (blockIdx%x-1)*blockDim%x

       if (i <= imax) then
              !Computation of the bottom friction
       endif

end subroutine
```

References

Béjar, M., Vericat, D., Nogales, I., Gallart, F., Batalla, R.J., 2018. Efectos de las extracciones de áridos sobre el transporte de sedimentos en suspensión en ríos de montaña (alto río Cinca, Pirineo Central). Cuadernos Invest. Geogr. 44, 641–658. https://doi.org/10.18172/cig.3256.

Benjankar, R., Tonina, D., McKean, J.A., Sohrabi, M.M., Chen, Q., Vidergar, D., 2018. Dam operations may improve aquatic habitat and offset negative effects of climate change. J. Environ. Manag. 213, 126–134. https://doi.org/10.1016/j.jenvman.2018.02.066.

Bermúdez, M., Cea, L., Puertas, J., Conde, A., Martín, A., Baztán, J., 2017. Hydraulic model study of the intake-outlet of a pumped-storage hydropower plant. Eng. Appl. Comput. Fluid Mech. 11, 483–495. https://doi.org/10.1080/19942060.2017.1314869.

Bermúdez, M., Cea, L., Puertas, J., Rodríguez, N., Baztán, J., 2018. Numerical modeling of the impact of a pumped-storage hydroelectric power plant on the reservoirs' thermal stratification structure: a case study in NW Spain. Environ. Model. Assess. 23, 71–85. https://doi.org/10.1007/s10666-017-9557-3.

Bermúdez, M., Puertas, J., Cea, L., Pena, L., Balairón, L., 2010. Influence of pool geometry on the biological efficiency of vertical slot fishways. Ecol. Eng. 36, 1355–1364. https://doi.org/10.1016/j.ecoleng.2010.06.013.

Bladé, E., Cea, L., Corestein, G., 2014a. Numerical modelling of river inundations [in Spanish]. Ing. del agua 18, 68. https://doi.org/10.4995/ia.2014.3144.

Bladé, E., Cea, L., Corestein, G., Escolano, E., Puertas, J., Vázquez-Cendón, E., Dolz, J., Coll, A., 2014b. Iber: river flow numerical simulation tool [in Spanish]. Rev. Int. Métodos Numéricos Cálculo Diseño Ing. 30, 1–10. https://doi.org/10.1016/j.rimni.2012.07.004.

Bladé, E., Sánchez-Juny, M., Arbat, M., Dolz, J., 2019a. Computational modeling of fine sediment relocation within a dam reservoir by means of artificial flood generation in a reservoir cascade. Water Resour. Res. 55, 3156–3170. https://doi.org/10.1029/2018WR024434.

Bladé, E., Sanz-Ramos, M., Dolz, J., Expósito-Pérez, J., Sánchez-Juny, M., 2019b. Modelling flood propagation in the service galleries of a nuclear power plant. Nucl. Eng. Des. 352, 110180 https://doi.org/10.1016/j.nucengdes.2019.110180.

Boudreault, J., Bergeron, N.E., St-Hilaire, A., Chebana, F., 2022. A new look at habitat suitability curves through functional data analysis. Ecol. Model. 467, 109905 https://doi.org/10.1016/j.ecolmodel.2022.109905.

Bovee, K.D., 1982. A guide to stream habitat analysis using the Instream Flow Incremental Methodology. Instream Flow Information, FWS/OBS¬82/26, 12, p. 248. Fort Collins, Color.

Buttinger-Kreuzhuber, A., Konev, A., Horváth, Z., Cornel, D., Schwerdorf, I., Blöschl, G., Waser, J., 2022. An integrated GPU-accelerated modeling framework for high-resolution simulations of rural and urban flash floods. Environ. Model. Software 156, 105480. https://doi.org/10.1016/j.envsoft.2022.105480.

Carlotto, T., Borges Chaffe, P.L., Innocente dos Santos, C., Lee, S., 2021. SW2D-GPU: a two-dimensional shallow water model accelerated by GPGPU. Environ. Model. Software 145, 105205. https://doi.org/10.1016/j.envsoft.2021.105205.

Cassan, L., Roux, H., Courret, D., Richard, S., 2022. Sensitivity of aquatic habitat modeling to hydrodynamic calibration. J. Ecohydraulics 1–9. https://doi.org/10.1080/24705357.2022.2049014.

Cea, L., Bermúdez, M., Puertas, J., Bladé, E., Corestein, G., Escolano, E., Conde, A., Bockelmann-Evans, B., Ahmadian, R., 2016. IberWQ: new simulation tool for 2D water quality modelling in rivers and shallow estuaries. J. Hydroinf. 18, 816–830. https://doi.org/10.2166/hydro.2016.235.

Cea, L., Bladé, E., 2015. A simple and efficient unstructured finite volume scheme for solving the shallow water equations in overland flow applications. Water Resour. Res. 51, 5464–5486. https://doi.org/10.1002/2014WR016547.

Cea, L., Bladé, E., Sanz-Ramos, M., Fraga, I., Sañudo, E., García-Feal, O., Gómez-Gesteira, M., González-Cao, J., 2010. Benchmarking of the Iber Capabilities for 2D Free Surface Flow Modelling. Universidade da Coruña. Servizo de Publicacións. https://doi.org/10.17979/spudc.9788497497640.

Cea, L., Pena, L., Puertas, J., Vázquez-Cendón, M.E., Peña, E., 2007. Application of several depth-averaged turbulence models to simulate flow in vertical slot fishways. J. Hydraul. Eng. 133, 160–172. https://doi.org/10.1061/(ASCE)0733-9429(2007)133:2(160).

CHE, 2021. SAIH Ebro [WWW Document]. Confed. Hidrográfica del Ebro. http://www.saihebro.com. accessed 3.15.21.

CHE, 2002. Study of the Integral Ecological Quality of the Most Important Fluvial Sections of the Cinca River, vol. III (in Spanish).

CHE, ACA, 2008. Evaluation of Environmental Flows and Biological Validation in Significant Sections of the River Network of Catalonia (in Spanish).

García-Feal, O., González-Cao, J., Gómez-Gesteira, M., Cea, L., Domínguez, J., Formella, A., 2018. An accelerated tool for flood modelling based on iber. Water 10, 1459. https://doi.org/10.3390/w10101459.

Hamilton, S.H., Pollino, C.A., Jakeman, A.J., 2015. Habitat suitability modelling of rare species using Bayesian networks: model evaluation under limited data. Ecol. Model. 299, 64–78. https://doi.org/10.1016/j.ecolmodel.2014.12.004.

Hung, H.-J., Lo, W.-C., Chen, C.-N., Tsai, C.-H., 2022. Fish' habitat area and habitat transition in a river under ordinary and flood flow. Ecol. Eng. 179, 106606 https://doi.org/10.1016/j.ecoleng.2022.106606.

Hwu, W.-M., Rodrigues, C., Ryoo, S., Stratton, J., 2009. Compute unified device architecture application suitability. Comput. Sci. Eng. 11, 16–26. https://doi.org/10.1109/MCSE.2009.48.

IGN, 2022. Digital Elevation Models [WWW Document]. Cent. Descargas. http://centrodedescargas.cnig.es/CentroDescargas/. accessed 4.26.22.

IGN, 2021. Ortofotos e imágenes satélite [WWW Document]. Cent. Descargas. http://centrodedescargas.cnig.es/CentroDescargas/catalogo.do?Serie=PNOAH. accessed 4.6.21.

Jowett, I.G., 2004. RHYHABSIM river hydraulics and habitat simulation computer manual. Software Manual 3.2 version 77.

Martinez, F., 2000. Régimen Ambiental De Caudales: Estimación De Las Condiciones De Habitabilidad Para La Ictiofauna, pp. 1–19.

Meselhe, E.A., Georgiou, I., Allison, M.A., McCorquodale, J.A., 2012. Numerical modeling of hydrodynamics and sediment transport in lower Mississippi at a proposed delta building diversion. J. Hydrol. 472–473, 340–354. https://doi.org/10.1016/j.jhydrol.2012.09.043.

Meza Rodríguez, D., Martinez Rivera, L.M., Olguín López, J.L., Aguirre García, Á., 2019. Simulation of physical habitat in Ayuquila-Armeria river in the west of Mexico. Cienc. e Ing. Neogranadina 29, 53–68. https://doi.org/10.18359/rcin.3128.

Morales-Hernández, M., Sharif, M.B., Kalyanapu, A., Ghafoor, S.K., Dullo, T.T., Gangrade, S., Kao, S.-C., Norman, M.R., Evans, K.J., 2021. TRITON: a Multi-GPU open source 2D hydrodynamic flood model. Environ. Model. Software 141, 105034. https://doi.org/10.1016/j.envsoft.2021.105034.

Narumi, T., Hamada, T., Nitadori, K., Sakamaki, R., Yasuoka, K., 2011. Fast quasi double-precision method with single-precision hardware to accelerate scientific applications. Int. J. Comput. Methods 8, 561–581. https://doi.org/10.1142/S0219876211002708.

Néelz, S., Pender, G., 2013. Benchmarking the Latest Generation of 2D Hydraulic Modelling Packages. Report - SC120002. Environment Agency, Horison House, Deanery Road, Bristol, BS1 9AH.

Nestler, J.M., Stewardson, M.J., Gilvear, D.J., Webb, J.A., Smith, D.L., 2016. Ecohydraulics exemplifies the emerging "paradigm of the interdisciplines. J. Ecohydraulics 1, 5–15. https://doi.org/10.1080/24705357.2016.1229142.

Nones, M., 2019. Numerical Modelling as a Support Tool for River Habitat Studies: an Italian Case Study, vol. 11. https://doi.org/10.3390/w11030482. Water (Switzerland).

NVIDIA, 2022a. NVIDIA HPC SDK Version 22.3 Documentation [WWW Document]. URL. https://docs.nvidia.com/hpc-sdk/compilers/. accessed 2.25.22.

NVIDIA, 2022b. NVIDIA CUDA Fortran Programming Guide [WWW Document]. URL. https://docs.nvidia.com/hpc-sdk/compilers/cuda-fortran-prog-guide/. accessed 2.23.22.

Palau, A., Alcázar, J., 2012. The basic flow method for incorporating flow variability in environmental flows. River Res. Appl. 28, 93–102. https://doi.org/10.1002/rra.1439.

Palau, A., Alcázar, J., Rocaspana, R., Aparicio, E., Mariño, F., 2016. Misusing physical habitat assessment techniques for environmental flows calculations. In: Proceedings of 11th International Symposium on Ecohydraulics. Melbourne (Australia).

Pisaturo, G.R., Folegot, S., Menapace, A., Righetti, M., 2021. Modelling fish habitat influenced by sediment flushing operations from an Alpine reservoir. Ecol. Eng. 173, 106439 https://doi.org/10.1016/j.ecoleng.2021.106439.

Pisaturo, G.R., Righetti, M., Dumbser, M., Noack, M., Schneider, M., Cavedon, V., 2017. The role of 3D-hydraulics in habitat modelling of hydropeaking events. Sci. Total Environ. 575, 219–230. https://doi.org/10.1016/j.scitotenv.2016.10.046.

Puertas, J., Cea, L., Bermúdez, M., Pena, L., Rodríguez, Á., Rabuñal, J.R., Balairón, L., Lara, Á., Aramburu, E., 2012. Computer application for the analysis and design of vertical slot fishways in accordance with the requirements of the target species. Ecol. Eng. 48, 51–60. https://doi.org/10.1016/j.ecoleng.2011.05.009.

Puertas, J., Pena, L., Teijeiro, T., 2004. Experimental approach to the hydraulics of vertical slot fishways. J. Hydraul. Eng. 130, 10–23. https://doi.org/10.1061/(ASCE)0733-9429(2004)130:1(10).

Roe, P.L., 1986. A basis for the upwind differencing of the two-dimensional unsteady Euler equations. Numer. Methods Fluid Dyn. 2, 55–80.

Ruiz-Villanueva, V., Bladé, E., Sánchez-Juny, M., Marti-Cardona, B., Díez-Herrero, A., Bodoque, J.M., 2014. Two-dimensional numerical modeling of wood transport. J. Hydroinf. 16, 1077. https://doi.org/10.2166/hydro.2014.026.

Sanz-Ramos, M., Bladé, E., Escolano, E., 2020a. Optimización del cálculo de la Vía de Intenso Desagüe con criterios hidráulicos. Ing. del agua 24, 203. https://doi.org/10.4995/ia.2020.13364.

Sanz-Ramos, M., Bladé, E., González-Escalona, F., Olivares, G., Aragón-Hernández, J.L., 2021. Interpreting the Manning roughness coefficient in overland flow simulations with coupled hydrological-hydraulic distributed models. Water 13, 3433. https://doi.org/10.3390/w13233433.

Sanz-Ramos, M., Bladé, E., Palau, A., Vericatl, D., Ramos-Fuertes, A., 2019. IberHABITAT: assessment of physical habitat suitability and weighted useable area for fishes. Application in the Eume River. Ribagua 6, 158–167. https://doi.org/10.1080/23863781.2019.1664273.

Sanz-Ramos, M., Martí-Cardona, B., Bladé, E., Seco, I., Amengual, A., Roux, H., Romero, R., 2020b. NRCS-CN estimation from onsite and remote sensing data for management of a reservoir in the Eastern Pyrenees. J. Hydrol. Eng. 25, 05020022 https://doi.org/10.1061/(ASCE)HE.1943-5584.0001979.

Shim, T., Kim, Z., Seo, D., Kim, Y.-O., Hwang, S.-J., Jung, J., 2020. Integrating hydraulic and physiologic factors to develop an ecological habitat suitability model. Environ. Model. Software 131, 104760. https://doi.org/10.1016/j.envsoft.2020.104760.

Soares-Frazão, S., Zech, Y., 2007. Experimental study of dam-break flow against an isolated obstacle. J. Hydraul. Res. 45, 27–36. https://doi.org/10.1080/00221686.2007.9521830.

Stamou, A., Polydera, A., Papadonikolaki, G., Martínez-Capel, F., Muñoz-Mas, R., Papadaki, C., Zogaris, S., Bui, M.D., Rutschmann, P., Dimitriou, E., 2018. Determination of environmental flows in rivers using an integrated hydrological-hydrodynamic-habitat modelling approach. J. Environ. Manag. 209, 273–285. https://doi.org/10.1016/j.jenvman.2017.12.038.

Steffler, P., Blackburn, J., 2002. Two-dimensional depth averaged model of river hydrodynamincs and fish habitat. In: User Manual River2D. University of Alberta, Canada.

Tonina, D., Jorde, K., 2013. Approaches for ecohydraulic non-numerical models. Ecohydraulics An Integr. Approach 31–74.

Toro, E.F., 2009. Riemann Solvers and Numerical Methods for Fluid Dynamics. Springer, Berlin/Heidelberg, Germany. https://doi.org/10.1007/b79761.

Vacondio, R., Dal Palù, A., Mignosa, P., 2014. GPU-enhanced finite volume shallow water solver for fast flood simulations. Environ. Model. Software 57, 60–75. https://doi.org/10.1016/j.envsoft.2014.02.003.

Vericat, D., Wheaton, J.M., Brasington, J., 2017. Revisiting the morphological approach. In: Gravel-Bed Rivers. John Wiley & Sons, Ltd, Chichester, UK, pp. 121–158. https://doi.org/10.1002/9781118971437.ch5.

Wang, F., Lin, B., 2013. Modelling habitat suitability for fish in the fluvial and lacustrine regions of a new Eco-City. Ecol. Model. 267, 115–126. https://doi.org/10.1016/j.ecolmodel.2013.07.024.

Wilkes, M.A., Neverman, A.J., Casas-Mulet, R., Adeva-Bustos, A., McCluskey, A.H., Ouellet, V., Vanzo, D., Franklin, P.A., Silva, A.T., 2016. Early careers on ecohydraulics: challenges, opportunities and future directions. J. Ecohydraulics 1, 102–107. https://doi.org/10.1080/24705357.2016.1249423.

Zhang, Y., Jia, Y., 2013. Parallelized CCHE2D flow model with CUDA fortran on graphics processing units. Comput. Fluids 84, 359–368. https://doi.org/10.1016/j.compfluid.2013.06.021.

Zohmann, M., Pennerstorfer, J., Nopp-Mayr, U., 2013. Modelling habitat suitability for alpine rock ptarmigan (Lagopus muta helvetica) combining object-based classification of IKONOS imagery and Habitat Suitability Index modelling. Ecol. Model. 254, 22–32. https://doi.org/10.1016/j.ecolmodel.2013.01.008.